$(\gamma,2e)$ total and differential cross-section calculations for helium at various excess energies

J. Colgan and M. S. Pindzola
Department of Physics, Auburn University, Auburn, Alabama 36849
(Received 28 September 2001; published 1 March 2002)

There have recently been several relative measurements of triple differential cross sections for the double photoionization of helium by a number of various experimental groups. In response to these measurements, we present theoretical calculations of total integral, single differential, and triple differential cross sections for this process using the time-dependent close-coupling method. This approach has previously given excellent agreement with absolute experimental measurements [see Colgan *et al.*, J. Phys. B **34** L457 (2001)]. Detailed comparisons with the experimental measurements are made, where possible, and, in general, very good agreement is found with the relative experiments over a wide range of excess energies and ejected electron energies and angles.

DOI: 10.1103/PhysRevA.65.032729 PACS number(s): 32.80.Fb, 34.80.Kw

I. INTRODUCTION

The double photoionization of helium remains the classic case that best summarizes the problems presented in the description of three interacting charged particles. Consequently, there has been much recent work describing the double photoionization of helium from both a theoretical and experimental approach. From a theoretical perspective, there has been several encouraging developments in recent years that have made much progress in describing the three-body Coulomb problem inherent in the double photoionization of helium. Total and angular differential cross sections for the double photoionization of helium have been calculated using the double screened Coulomb [1–3] and the hyperspherical *R*-matrix [4,5] methods. The converged close-coupling (CCC) [6,7] and the time-dependent close-coupling methods [8,9] have also successfully calculated the total integral and angular differential cross sections for helium as well as the related two-electron problem of the double photoionization of beryllium [10,11].

Much experimental work on this process has also been reported. Absolute total double photoionization cross sections have been measured [12] as well as absolute single differential cross sections at an excess energy of 20 eV [13]. Dörner and co-workers [14,15] have used the well-known recoil-ion-momentum-spectroscopy technique to measure absolute triple differential cross sections for helium at 20 eV excess energy, measurements that are in excellent agreement with *ab initio* calculations [9]. There have also been many other experiments that have focused solely on the triple differential cross sections arising from the double photoionization process. The triple differential cross section remains the most critical test of experiment and theory since it is dependent on the ejected angles and energies of each of the outgoing electrons and thus provides a sensitive measure of the electron-electron correlation. Many measurements have been made of relative triple differential cross sections of helium [16,17] and D_2 [18,19] at various excess energies, with many different combinations of angle and energy sharing between the outgoing electrons. In this paper we compare the time-dependent close-coupling method with the most recent of these measurements and find, in general, very good agreement between experiment and theory. Other measurements have also been made [20] with very unequal energy-sharing conditions between the electrons for an excess energy of 40 eV. We compare with these experiments also, in an attempt to understand some differences between experiment and other theoretical calculations presented in Ref. [20]. The main experimental results in the study of two-electron processes and a comprehensive analysis of experimental and theoretical developments have been the subject of two recent reviews [21,22]; we refer the reader to these for a more detailed overview of the field.

In this paper we present total integral and single differential cross sections at various excess energies, and also present comparisons of triple differential cross sections with these recent experimental measurements. In Sec. II we give a brief description of the time-dependent close-coupling method and in Sec. III we present our results and comparisons with experiment. A summary is given in Sec. IV.

II. TIME-DEPENDENT CLOSE-COUPLING THEORY

The time-dependent close-coupling theory describing double-photoionization processes has been described in detail in previous work [8,9,11]. Here we give only a summary of the theory.

We begin with the time-dependent Schrödinger equation in real time,

$$i\frac{\partial \Psi^{1P}(\vec{r}_1,\vec{r}_2,t)}{\partial t} = H_{\rm atom}\Psi^{1P}(\vec{r}_1,\vec{r}_2,t) + H_{\rm rad}\Phi_0^{1S}(\vec{r}_1,\vec{r}_2)e^{-iE_0t}, \tag{1}$$

where the Hamiltonian for a linearly polarized radiation field in the length gauge is given by

$$H_{\rm rad} = E(t)(r_1\cos\theta_1 + r_2\cos\theta_2)\cos(\omega t), \tag{2}$$

with electric-field amplitude $E(t)$ and radiation frequency ω. The ground state of helium $\Phi_0^{1S}(\vec{r}_1,\vec{r}_2)$ is found by an expansion in coupled spherical harmonics and subsequent relaxation of the time-dependent Schrödinger equation (containing only the nonrelativistic Hamiltonian $H_{\rm atom}$) in imaginary

time. The electric field is ramped on smoothly over one quarter of a field period so that $E(t)=t/T$ for $t<T/4$, $E(t)=1$ for $t>T/4$. The velocity gauge may also be used, but previous time-dependent close-coupling calculations [8] for the double-photoionization cross sections of helium have been found to be gauge invariant.

The time-dependent wave function $\Psi^{^1P}(\vec{r}_1,\vec{r}_2,t)$ is also expanded in coupled spherical harmonics and the resulting set of coupled partial differential equations are solved on a numerical lattice with a mesh spacing of $\Delta r=0.1$ and time propagated for between 10 and 15 radiation field periods $(2\pi/\omega)$, depending on the excess photon energy. A lattice size of 600×600 points is employed. Increasing the lattice to 1000×1000 points made a difference of no more than 2% in any of the results presented here.

The total integral cross section for double photoionization is given by

$$\sigma_{\rm dion}=\frac{\omega}{I}\frac{\partial\mathcal{P}_{\rm dion}}{\partial t}, \tag{3}$$

where I is the radiation field intensity, and $\mathrm{P}_{\rm dion}$ is the probability for double ionization defined by

$$\mathcal{P}_{\rm dion}=\sum_{l_1,l_2}\frac{2}{\pi}\int dk_1\frac{2}{\pi}\int dk_2|P^{^1P}_{l_1l_2}(k_1,k_2,t)|^2, \tag{4}$$

where

$$P^{^1P}_{l_1l_2}(k_1,k_2,t)=\int_0^\infty dr_1 \times\int_0^\infty dr_2 P_{k_1l_1}(r_1)P_{k_2l_2}(r_2)P^{^1P}_{l_1l_2}(r_1,r_2,t), \tag{5}$$

and $P^{^1P}_{l_1l_2}(r_1,r_2,t)$ are two-dimensional radial wave functions. The radial continuum states, $P_{kl}(r)$, are obtained on a fixed mesh in momentum space by integrating the radial Schrödinger equation for a Coulomb potential with $Z=2$ and normalizing to a sine function, for which $\Sigma_k\rightarrow(2/\pi)\int dk$. For most of the calculations presented here, 600 continuum-state radial orbitals on a uniform momentum mesh were used, with a mesh spacing of typically 0.0025. A slightly larger mesh spacing was sometimes used in order to span a larger energy range for larger excess energy calculations.

The ejected-energy differential cross section may be defined as

$$\frac{d\sigma}{dE_1}=\frac{1}{k_1k_2}\frac{d\sigma}{d\alpha}, \tag{6}$$

where $d\sigma/d\alpha$ is the angle differential cross section in hyperspherical angle and integration of the differential cross section over all excess energy gives the total integral cross section. We remark here that this convention is different from the most commonly used convention where the ejected-energy differential cross section is defined from 0 to $E/2$.

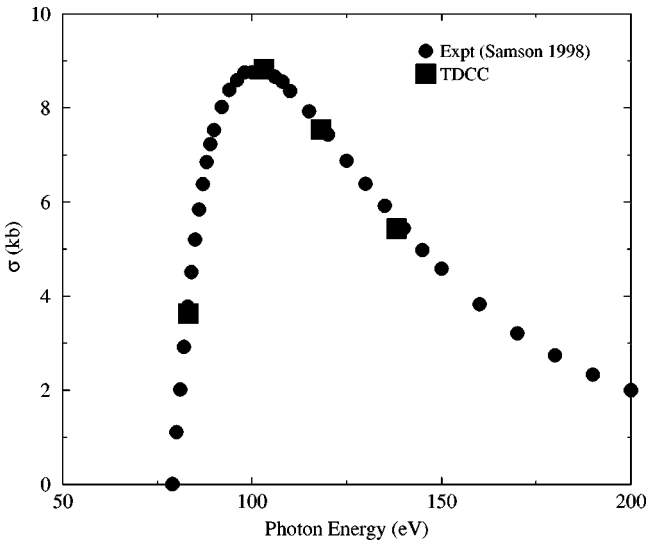

FIG. 1. Total double-photoionization cross section in kilobarn for helium. The solid squares are the time-dependent close-coupling results and the solid circles are the experimental measurements of Samson *et al.* [12]. (1.0 kb$=1.0\times10^{-21}$ cm^2.)

The triple differential cross section for double photoionization is given by

$$\frac{d^3\sigma}{d\alpha d\Omega_1 d\Omega_2}=\frac{\omega}{I}\frac{\partial}{\partial t}\frac{2}{\pi}\int_0^\infty dk_1\frac{2}{\pi}\int_0^\infty dk_2\delta\left[\alpha-\tan^{-1}\left(\frac{k_2}{k_1}\right)\right] \times\left|\sum_{l_1,l_2} i^{l_1+l_2}e^{i(\sigma_{l_1}+\sigma_{l_2})} \times P^{^1P}_{l_1l_2}(k_1,k_2,t)Y^{^1P}_{l_1l_2}(\hat{k}_1,\hat{k}_2)\right|^2, \tag{7}$$

where σ_l is the Coulomb phase shift and $Y^{^1P}_{l_1l_2}(\hat{k}_1,\hat{k}_2)$ are coupled spherical harmonics, and integration over all solid angles and ejected energy gives the total integral cross section.

III. RESULTS

A. Total integral and single differential cross sections

Total integral double-photoionization cross sections have been calculated at 4, 25, 40, and 60 eV excess photon energy using the time-dependent close-coupling method. In Fig. 1 we compare these calculations to the absolute experimental measurements of Samson *et al.* [12]. The agreement between theory and experiment is excellent, reproducing the position and magnitude of the peak of the cross section. These calculations are also in excellent agreement with other theoretical calculations [3,5,7].

In Fig. 2 we present single differential cross-section calculations for helium at the same excess energies. For ease of presentation we plot the single differential cross sections against normalized ejected energy (i.e. ejected energy/excess energy). Unfortunately, at these energies, there are no absolute experimental measurements available with which to

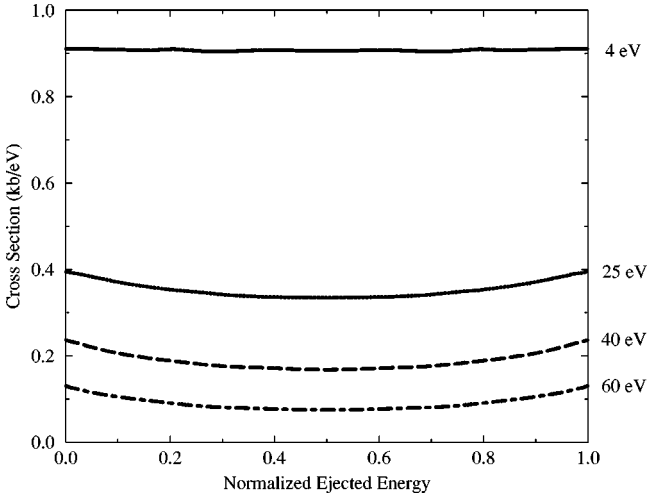

FIG. 2. Single energy differential cross section in kb/eV for helium at various excess photon energies as indicated. The cross sections are normalized such that the normalized ejected energy = ejected energy/excess energy. (1.0 kb $=1.0\times10^{-21}$ cm^2.)

compare. We have previously shown excellent agreement [9] with other experimental measurements [13] at an excess energy of 20 eV. As expected, the single differential cross section is flat for low excess energies and becomes progressively more ''smile shaped'' at higher energies. In this convention it is clear that the area under the curve multiplied by the excess energy gives the total integral cross section. This is a different convention than that used in our previous paper [9] on helium at 20 eV, where the single differential cross section was presented in such a way that the area under the curve from 0 to $E/2$ yielded the total integral cross section, in order to compare with experiment.

B. Triple differential cross sections at 25 eV excess energy: Comparisons with Collins *et al.* [19]

We now turn our attention to comparisons with recent experimental measurements of relative triple differential cross sections. Collins *et al.* [19] performed experiments at the Super-ACO synchrotron in France for an excess energy of 25 eV, where they measured the triple differential cross section for various unequal energy sharing cases. In this and all subsequent figures, results are presented for the case of coplanar geometry ($\phi_1=\phi_2=0$).

Figure 3 shows triple differential cross sections at an excess energy of 25 eV for the unequal energy sharing case of E_1 (the energy of the first ejected electron) equal to 5 eV and E_2 (the energy of the second ejected electron) equal to 20 eV, for various different angles of the first electron, as shown. For this and all successive figures, the solid lines are the time-dependent close-coupling calculations and the solid circles are the experimental measurements. The experimental measurements for $\theta_1=0°$, 10°, and 20° have all been normalized to the time-dependent calculations at $\theta_1=0°$. The $\theta_1=90°$ measurements have been independently normalized to the time-dependent results since the measurements at this angle are taken from coincidence measurements between two different analyzers than for the other angles (see Ref. [19] for more details). It is clear that the agreement between the absolute theoretical calculations and the experimental results are very good. In all cases theory reproduces the position and magnitude of the peaks in the triple differential cross section over a wide range of angles.

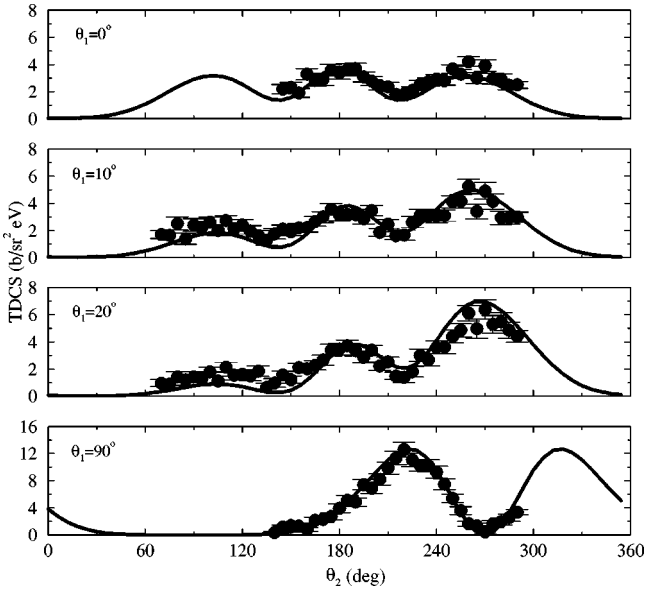

FIG. 3. Triple differential cross section in b/sr^2 eV for helium at an excess energy of 25 eV, for various values of θ_1, the ejected angle of the first electron, over a range of θ_2, the ejected angle of the second electron. The energy of the first electron (E_1) is 5 eV and the second electron (E_2) has 20 eV. The solid lines are the time-dependent close-coupling calculations and the solid circles are the experimental results of Collins *et al.* [19]. The experimental measurements have been normalized to the absolute time-dependent calculations at $\theta_1=0°$ except for the $\theta_1=90°$ measurements that are independently normalized (see text). (1.0 b $=1.0\times10^{-24}$ cm^2.)

C. Triple differential cross sections at 40 eV excess energy: Comparisons with Cvejanović *et al.* [16]

Cvejanović *et al.* [16] recently carried out coincidence experiments at the Daresbury Synchrotron Radiation Source in Warrington, England. Extensive measurements were made of triple differential cross sections at an excess energy of 40 eV, for a wide range of energy and angle sharings between the electrons. In Figs. 4–7 we compare these measurements to calculations using the time-dependent method.

In Fig. 4 we compare the triple differential cross sections for equal energy sharing between the electrons for various values of θ_1 as shown. The experimental measurements are normalized to the time-dependent calculations at $\theta_1=95°$. Again the agreement between experiment and theory is excellent. The large forward peak in the cross section mapped out by experiment is completely reproduced in position and magnitude by theory. We remark here also that comparisons are made in Ref. [16] with other CCC calculations that are also in excellent agreement with the experimental results.

Figure 5 shows triple differential cross sections for the unequal energy-sharing case of $E_1=10$ eV, $E_2=30$ eV for

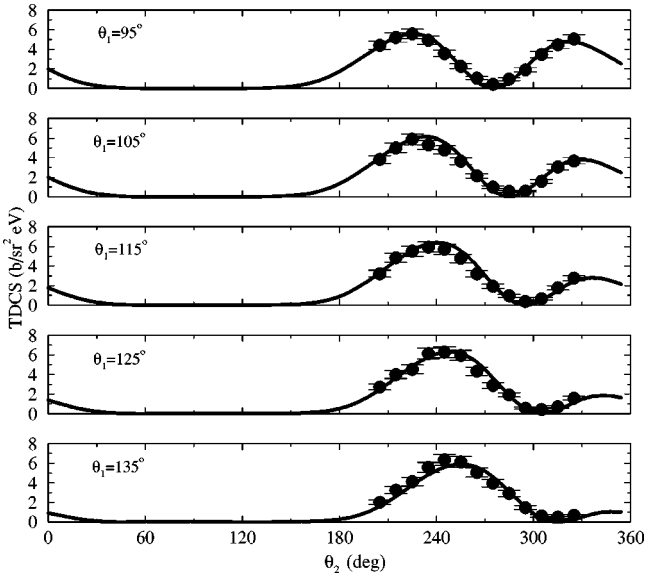

FIG. 4. Triple differential cross section in b/sr^2 eV for helium at an excess energy of 40 eV for various values of θ_1 as shown. The excess energy is shared equally between the two ejected electrons. The solid lines are the time-dependent close-coupling calculations and the solid circles are the experimental results of Cvejanović *et al.* [16]. The experimental measurements are normalized to the time-dependent calculations at $\theta_1=95°$. (1.0 b$=1.0\times10^{-24}$ cm^2.)

various values of θ_1 as shown. The experimental data are normalized to the time-dependent calculations at $\theta_1=90°$. The agreement between theory and experiment in all respects is still very good. Figure 6 shows similar calculations at higher values of θ_1 as shown, for the same energy-sharing conditions. We now plot the value of θ_2 from $-180°$ to

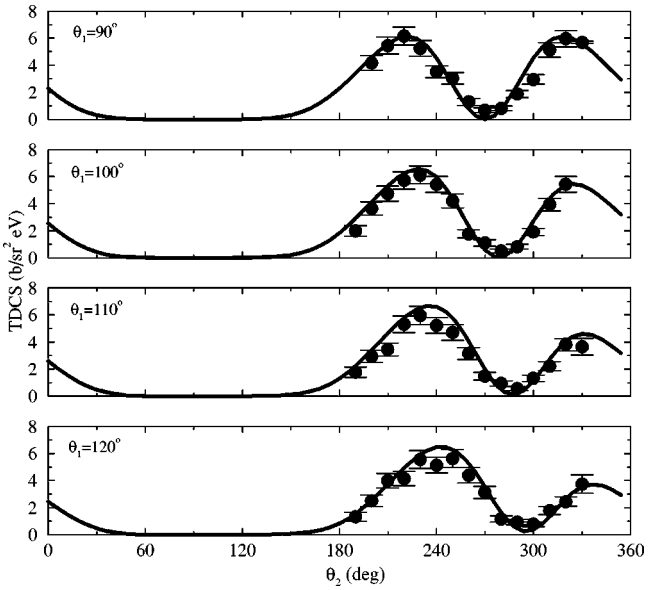

FIG. 5. Same as Fig. 4 for the case of $E_1=10$ eV, $E_2=30$ eV, for various values of θ_1 as shown. The experimental measurements are normalized to the time-dependent calculations at $\theta_1=90°$. (1.0 b$=1.0\times10^{-24}$ cm^2.)

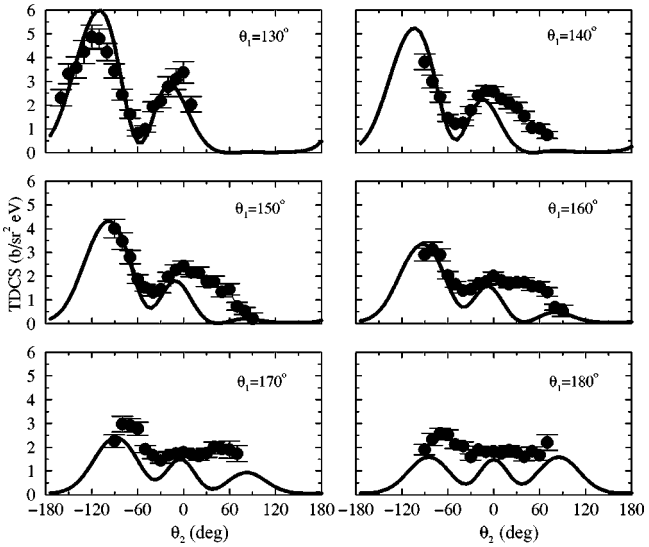

FIG. 6. Same as Fig. 4 for the case of $E_1=10$ eV, $E_2=30$ eV, for various values of θ_1 as shown. The experimental measurements are normalized to the time-dependent calculations at $\theta_1=90°$. (1.0 b$=1.0\times10^{-24}$ cm^2.)

$+180°$ to show more clearly the trend in the experimental measurements, which now extend into the region above $\theta_2=0°$. The experimental measurements are still normalized to the time-dependent calculations at $\theta_1=90°$. Here the agreement between theory and experiment is not as spectacular as previously. Indeed, as θ_1 becomes larger the agreement in magnitude becomes poorer, although the positions of the peaks in the cross sections are still well reproduced. The experimental results also show an increasing ''shoulder'' on the secondary peak, most clearly for $\theta_1=150°$ and 160°, which is not found in the time-dependent calculations. We remark that the CCC results quoted in Ref. [16] display the

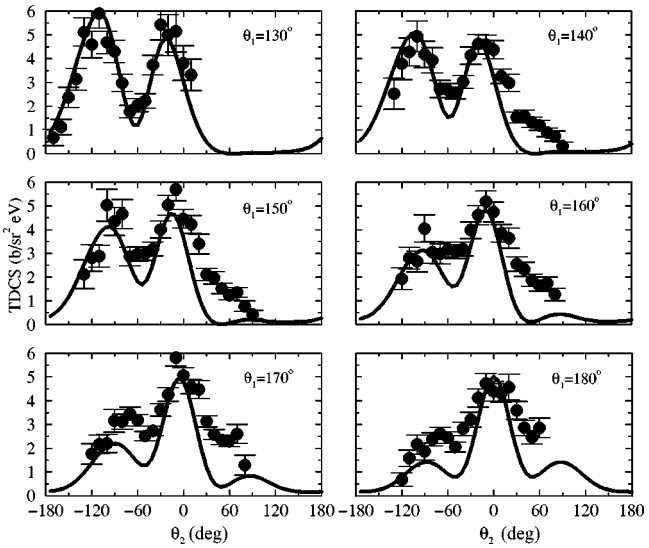

FIG. 7. Same as Fig. 4 for the case of $E_1=5$ eV, $E_2=35$ eV, for various values of θ_1 as shown. The experimental measurements are normalized to the time-dependent calculations at $\theta_1=130°$. (1.0 b$=1.0\times10^{-24}$ cm^2.)

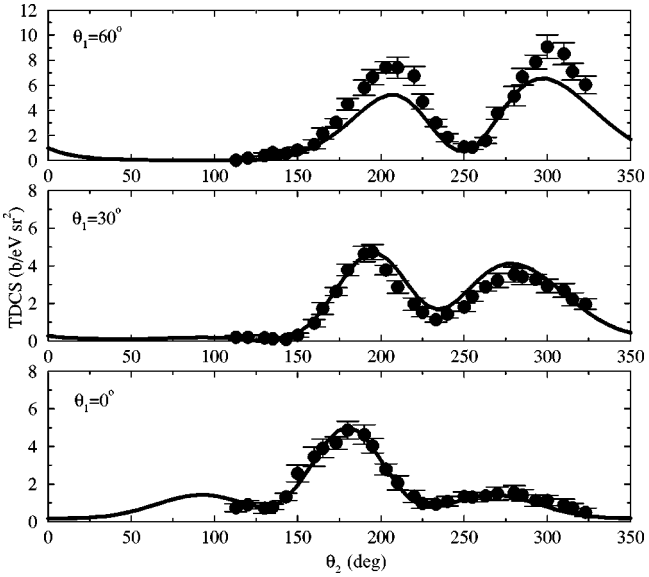

FIG. 8. Triple differential cross section in b/sr^2 eV for helium at an excess energy of 40 eV for various values of θ_1 as shown. The first electron has 5 eV and the second electron 35 eV of the total ejected energy. The solid lines are the time-dependent close-coupling calculations and the solid circles are the experimental results of Bolognesi *et al.* [20]. The normalization of the experimental measurements is the same as that adopted in Ref. [20] where they are normalized to CCC calculations at $\theta_1=60°$. (1.0 b$=1.0\times10^{-24}$ cm^2.)

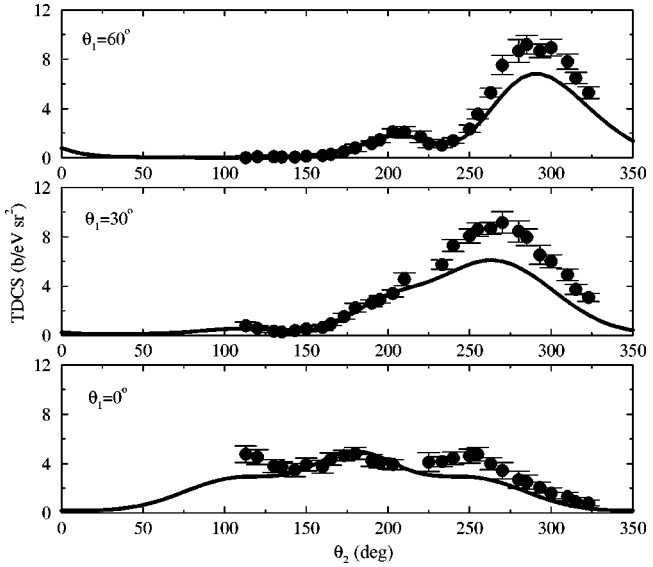

FIG. 9. Same as Fig. 8, for the case where the first electron has 35 eV and the second electron has 5 eV of the total ejected energy. (1.0 b$=1.0\times10^{-24}$ cm^2.)

same discrepancies with experiment and are in good agreement with these time-dependent results.

For the same angles, but different energy-sharing conditions ($E_1=5$ eV, $E_2=35$ eV), Fig. 7 compares the time-dependent calculations with the triple differential cross-section measurements of Ref. [16]. The experimental measurements have been normalized to the time-dependent measurements at $\theta_1=130°$. For this most extreme of energy-sharing conditions, the agreement between theory and experiment is good. Only in a few cases do the magnitudes of the peaks of the cross sections disagree, and in all cases the positions of the cross-section peaks are reproduced.

D. Triple differential cross sections at 40 eV excess energy: Comparisons with Bolognesi *et al.* [20]

In Figs. 8 and 9 we compare time-dependent calculations with a set of experimental measurements from Bolognesi *et al.* [20]. These experiments, using the Elettra storage ring in Italy, measured the triple differential cross sections for helium at 40 eV excess energy, for unequal energy-sharing conditions. The experimental measurements were compared with a practical parameterization fit obtained from Cvejanović and Reddish [23] and also with theoretical calculations using CCC theory. For some electron angles and energy-sharing conditions, quite large differences were found between experiment and CCC theoretical calculations.

In Fig. 8 we present triple differential cross sections for $E_1=5$ eV and $E_2=35$ eV. The normalization of the experimental measurements is the same as that quoted in Ref. [20], i.e. to the CCC calculations at $\theta_1=0°$. We see that there is generally very good agreement between the experimental measurements and the time-dependent calculations, although the experimental measurements give higher peaks in the cross section for $\theta_1=60°$.

In Fig. 9 we present the converse case: where $E_1=35$ eV and $E_2=5$ eV. Again we note that the experimental measurements have higher peaks in the cross section for $\theta_1=30°$ and 60°. However, it is clear that the shape of the triple differential cross sections is the same for both theory and experiment. This is in contrast to the CCC calculations for $\theta_1=0°$, where CCC predicts a much larger central peak in the cross section [20]. For $\theta_1=30°$, CCC also predicts a shoulder in the cross section around $\theta_2=210°$, which is not seen in either the experimental measurements or the time-dependent calculations. We do point out that CCC seems to be in good agreement with the experimental measurements for the $\theta_1=60°$ case.

E. Triple differential cross sections at 60 eV excess energy: Comparisons with Dawson *et al.* [17]

Very recently, Dawson *et al.* [17] carried out coincidence experiments on the Super-ACO storage ring in France where they examined the double-photoionization yield at an excess photon energy of 60 eV. In Figs. 10–12 we compare with these recent experimental measurements, which were made for a variety of equal and unequal energy-sharing cases.

Figure 10 shows triple differential cross sections for equal energy sharing between the outgoing electrons, for various values of θ_1 as shown. The experimental measurements are normalized to the time-dependent calculations at $\theta_1=90°$. The agreement between theory and experiment for this case is again excellent. The two peaks of the cross section are reproduced in both magnitude and position.

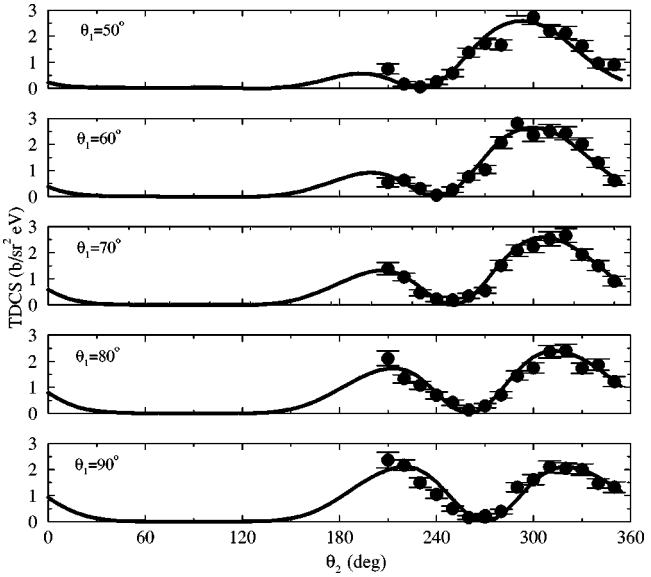

FIG. 10. Triple differential cross section in b/sr^2 eV for helium at an excess energy of 60 eV for various values of θ_1 as shown. The excess energy is shared equally between the two ejected electrons. The solid lines are the time-dependent calculations and the solid circles are the experimental measurements of Dawson *et al.* [17]. The experimental measurements are normalized to the time-dependent calculations at $\theta_1=90°$. (1.0 b$=1.0\times10^{-24}$ cm^2.)

Figure 11 compares the experimental measurements with the theoretical calculations for the unequal energy-sharing case, ($E_1=10$ eV, $E_2=50$ eV). In this case the experimental measurements are normalized to theory at $\theta_1=30°$. The agreement between theory and experiment is again very good. The three lobe structure expected is observed for all values of θ_1, although by $\theta_1=30°$ the lobe near 90° has almost disappeared. Similar calculations were made at the same angles for the extreme unequal energy sharing case of $E_1=5$ eV, $E_2=55$ eV, as shown in Fig. 12. The normalization is the same as in Fig. 11 and we see the very good agreement between theory and experiment. We remark also that our calculations, at all combinations of angles and energy sharings are very similar to the CCC results quoted in Ref. [17].

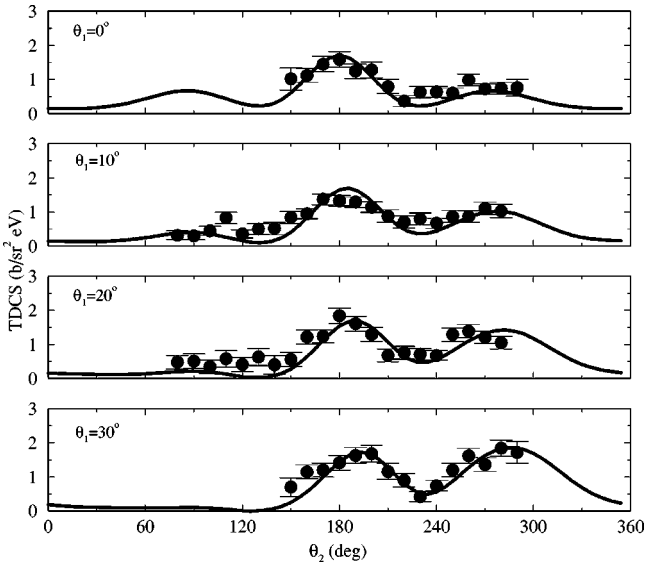

FIG. 11. Same as Fig. 10 for the case of $E_1=10$ eV, $E_2=50$ eV, for various values of θ_1 as shown. The solid lines are the time-dependent calculations and the solid circles are the experimental measurements of Dawson *et al.* [17]. The experimental measurements are normalized to the time-dependent calculations at $\theta_1=30°$. (1.0 b$=1.0\times10^{-24}$ cm^2.)

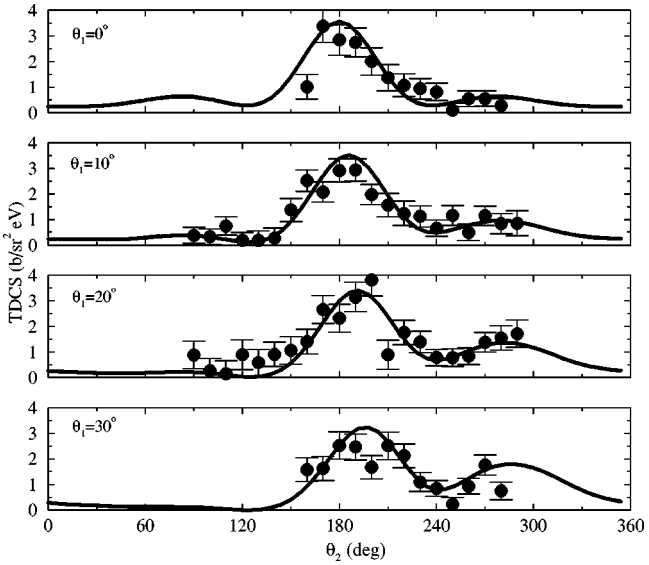

FIG. 12. Same as Fig. 10 for the case of $E_1=5$ eV, $E_2=55$ eV, for various values of θ_1 as shown. The solid lines are the time-dependent calculations and the solid circles are the experimental measurements of Dawson *et al.* [17]. The experimental measurements are normalized to the time-dependent calculations at $\theta_1=90°$. (1.0 b$=1.0\times10^{-24}$ cm^2.)

IV. SUMMARY

In summary, the time-dependent close-coupling method has been used to calculate total integral, single differential, and triple differential cross sections for the double photoionization of helium at various excess photon energies. This has been carried out in an effort to compare more closely with recent reports of measurements of relative triple differential cross sections by various groups. In general, excellent agreement is found between the theoretical calculations and the relative cross-sections measurements. The theoretical calculations are also in very good agreement with other nonperturbative calculations.

In previous work we have compared our calculations with absolute experimental measurements [9]. More extensive experimental measurements at an absolute level would enable more stringent tests of theory and experiment, especially for the areas for which theory and experiment prove most difficult, for example, the most unequal energy-sharing regions between the electrons. Also, there exists a major gap in absolute measurements of single differential cross sections. To our knowledge, only one such measurement has been carried out [13]. Although these experiments are very difficult, they also provide crucial tests of theory, especially in regard to the

shapes of the single differential cross sections close to threshold.

In future work, we aim to extend the time-dependent close-coupling method in a number of different directions. We have already calculated double-photoionization cross sections for beryllium [11] and hope to extend this to other alkaline earth systems. Also, work is already underway in calculating differential cross sections for $(2\gamma,2e)$ processes in helium, in support of planned experiments at the DESY Lab in Hamburg [23] involving a free-electron laser. It is hoped that such calculations can shed more light on the complex correlations involved in these two-electron systems.

ACKNOWLEDGMENTS

We would like to thank Tim Reddish and Lorenzo Avaldi for communication of their results in numerical form. This work was supported in part by the US Department of Energy. Computational work was carried out at the National Energy Research Supercomputing Center in Oakland, CA.

[1] D. Proulx and R. Shakeshaft, Phys. Rev. A **48**, R875 (1993).
[2] M. Pont, R. Shakeshaft, F. Maulbetsch, and J. S. Briggs, Phys. Rev. A **53**, 3671 (1996).
[3] M. Pont and R. Shakeshaft, J. Phys. B **28**, L571 (1995).
[4] L. Malegat, P. Selles, and A. K. Kazansky, Phys. Rev. A **60**, 3667 (1999).
[5] L. Malegat, P. Selles, and A. K. Kazansky, Phys. Rev. Lett. **85**, 4450 (2000).
[6] A. S. Kheifets and I. Bray, J. Phys. B **31**, L447 (1998).
[7] A. S. Kheifets and I. Bray, Phys. Rev. A **62**, 065402 (2000).
[8] M. S. Pindzola and F. Robicheaux, Phys. Rev. A **57**, 318 (1998); **58**, 779 (1998).
[9] J. Colgan, M. S. Pindzola, and F. Robicheaux, J. Phys. B **34**, L457 (2001).
[10] A. S. Kheifets and I. Bray, Phys. Rev. A **65**, 012710 (2001).
[11] J. Colgan and M. S. Pindzola, Phys. Rev. A **65**, 022709 (2002).
[12] J. A. R. Samson, W. C. Stolte, Z. X. He, J. N. Cutler, Y. Lu, and R. J. Bartlett, Phys. Rev. A **57**, 1906 (1998).
[13] R. Wehlitz, F. Heiser, O. Hemmers, B. Langer, A. Menzel, and U. Becker, Phys. Rev. Lett. **67**, 3764 (1991).
[14] R. Dörner, T. Vogt, V. Mergel, H. Klemliche, S. Kravis, C. L. Cocke, J. Ullrich, M. Unverzagt, L. Spielberger, M. Damrau, O. Jagutski, I. Ali, B. Weaver, K. Ullmann, C. C. Hsu, M. Jung, E. P. Kanter, B. Sonntag, M. H. Prior, E. Rotenberg, J. Denlinger, T. Warwick, S. T. Manson, and H. Schmidt-Böcking, Phys. Rev. Lett. **76**, 2654 (1996).
[15] H. Bräuning, R. Dörner, C. L. Cocke, M. H. Prior, B. Krassig, A. S. Kheifets, I. Bray, A. Bräuning-Demian, K. Carnes, S. Dreuil, V. Mergel, P. Richard, J. Ullrich, and H. Schmidt-Böcking, J. Phys. B **31**, 5149 (1998).
[16] S. Cvejanović, J. P. Wightman, T. J. Reddish, F. Maulbetsch, M. A. MacDonald, A. S. Kheifets, and I. Bray, J. Phys. B **33**, 265 (2000).
[17] C. Dawson, S. Cvejanović, D. Seccombe, T. J. Reddish, F. Maulbetsch, A. Huetz, J. Mazeau, and A. S. Kheifets, J. Phys. B **34**, L525 (2001).
[18] J. P. Wightman, S. Cvejanović, and T. J. Reddish, J. Phys. B **31**, 1753 (1998).
[19] S. A. Collins, A. Heutz, T. J. Reddish, D. P. Seccombe, and K. Soejima, Phys. Rev. A **64**, 062706 (2001).
[20] P. Bolognesi, R. Camilloni, M. Coreno, G. Turri, J. Berakdar, A. S. Kheifets, and L. Avaldi, J. Phys. B **34**, 3193 (2001).
[21] J. S. Briggs and V. Schmidt, J. Phys. B **33**, R1 (2000).
[22] G. C. King and L. Avaldi, J. Phys. B **33**, R215 (2000).
[23] S. Cvejanović and T. J. Reddish, J. Phys. B **33**, 4691 (2000).
[24] J. Andruszkow *et al.*, Phys. Rev. Lett. **85**, 3825 (2000).